Clustering of platinum atoms into nanoscale particle and network on NaY zeolite

Ryong Ryoo[1], Sung June Cho, Chanho Pak

Department of Chemistry and Center for Molecular Science, Korea Advanced Institute of Science and Technology, Taeduk Science Town, Taejon 305-701, Korea

and

Jeong Yong Lee

Department of Electronic Materials Science and Engineering, Korea Advanced Institute of Science and Technology, Taeduk Science Town, Taejon 305-701, Korea

Platinum has been supported on NaY zeolite by ion exchange of $Pt(NH_3)_4^{2+}$. Clustering of Pt atoms into a 1 nm cluster, and three-dimensional quantum-size wire (3 nm thick) network (greater than 100 nm) from reduction of the Pt species has been investigated by extended X-ray absorption fine structure transmission electron microscopy and xenon adsorption measurements.

Keywords: Pt cluster supported on zeolites; quantum-size Pt wire network; metal–support interaction; EXAFS; TEM

1. Introduction

Preparatory treatments affect critically the formation of Pt clusters from $Pt(NH_3)_4^{2+}$ exchanged on faujasite-type zeolite [1–6]. A small Pt cluster of about 1 nm in size is known to form in the supercage of the Y zeolite, when the reduction of Pt is performed with flowing H_2 at 573–673 K after the Pt species is activated in flowing O_2 at 573–673 K [2]. Pt reduction without the activation (or calcination) is reported to result in the formation of Pt particles of 10–50 nm in size due to migration of Pt onto the external surface of the zeolite crystal [3]. In this paper, we report the formation of Pt clusters which fill supercages (1.3 nm in diameter, with four apertures 0.74 nm in diameter) of NaY zeolite with very narrow distribution in the cluster size, using extended X-ray absorption fine structure (EXAFS) transmission electron microscopy (TEM), and xenon adsorption measurements. We also show

[1] To whom correspondence should be addressed.

the formation of a Pt network which probably starts at the external surface progressing into the zeolite crystal.

2. Experimental

$Pt(NH_3)_4^{2+}$ was ion exchanged into high-purity NaY zeolite by stirring the zeolite in an aqueous solution of $[Pt(NH_3)_4]Cl_2 \cdot H_2O$ (Johnson Matthey, Pt 56.4%) overnight at room temperature (RT). The zeolite was subsequently filtered, washed with doubly distilled water, and dried in a vacuum oven at 330 K. Such a precursor of Pt/NaY was subjected to the reduction of Pt by flowing H_2 (Korea Industrial Gas, 99.999%, further passed through a MnO/SiO_2 trap) at 200 ml g^{-1} without or after activation. For the activation, the sample was heated in flowing O_2 (Korea Industrial Gas, 99+%, >1 ℓ min^{-1} g^{-1}), in a pyrex U-tube reactor while the temperature was increased linearly from RT to 583 K over 12 h and further maintained at 583 K for 2 h. The reduction temperature was increased linearly from RT to 673 K over 2, 4 or 20 h, and subsequently maintained at this temperature for 2 h. Desorption of chemisorbed hydrogen from the surface of the Pt cluster, thus generated, was performed for 2 h under 1×10^{-5} Torr at 673 K. The sample was then used for xenon adsorption measurements in situ, or opened to air at RT before further use. The Pt content of the sample was determined by the difference in UV absorption of the supernatant solution which occurred due to the ion exchange of $Pt(NH_3)_4^{2+}$.

The xenon-adsorption isotherm was obtained by using a conventional volumetric gas adsorption apparatus. The adsorption temperature was controlled to within ± 0.1 K by a constant temperature circulation bath since the adsorption was very sensitive to the adsorption temperature. Air-exposed samples were reduced by flowing H_2 while the temperature was linearly increased from RT to 573 K over 2 h. The desorption of chemisorbed hydrogen was performed in the same way as used for the freshly prepared sample, before the adsorption of xenon (Matheson, 99.995%).

For EXAFS, the sample powder weighing 0.3, 0.2, and 0.1 g was pressed into disks of 10 mm in diameter for 2.0, 5.0, and 10.0 wt% Pt/NaY, respectively. The sample wafer was placed in a specially designed pyrex reactor which was jointed to an EXAFS cell with Kapton (Eastman Kodak) windows for the X-ray absorption measurement [7]. The reduction for the sample wafer was performed with flowing H_2 under the same condition used for the treatment of the air-exposed sample. After the sample wafer was transferred into the cell, the cell under a H_2 atmosphere was sealed off by flame. The EXAFS spectra were measured above the Pt L_{III} edge by using beamline 7C at the Photon Factory of the National Laboratory for High Energy Physics (KEK-PF) in Tsukuba, Japan.

For TEM, a suspension of the sample powder in methanol was dropped onto microporous carbon grid and allowed to dry. The micrographs of thin edges of the

zeolite crystal (~ 1 μm) were taken with a JEM 2000-EX (Jeol) apparatus operating at 200 keV.

3. Result and discussion

1 nm Pt Cluster. We have prepared 2–10 wt% Pt/NaY samples by ion exchange of $Pt(NH_3)_4^{2+}$ into NaY zeolite, subsequent activation in flowing O_2, and reduction in flowing H_2. The reduction temperature was linearly increased from RT to 573 K over 4 h, and further maintained at 573 K for 2 h. Fig. 1 shows EXAFS spectra weighted by cube of wave vector ($k^3\chi(k)$), and the Fourier transforms of the spectra. The Fourier transform was performed in the k range from 30 to 140 nm^{-1}. The radial distribution function thus obtained was inverse-Fourier transformed in the R range from 0.18 to 0.30 nm. Structural information on the Pt cluster, listed in table 1, has been estimated from curve fitting the Fourier filtered $k^3\chi(k)$ data, using a standard analysis and the experimental amplitude and phase shift from Pt foil as a reference. The coordination number for the nearest Pt–Pt pair coincides

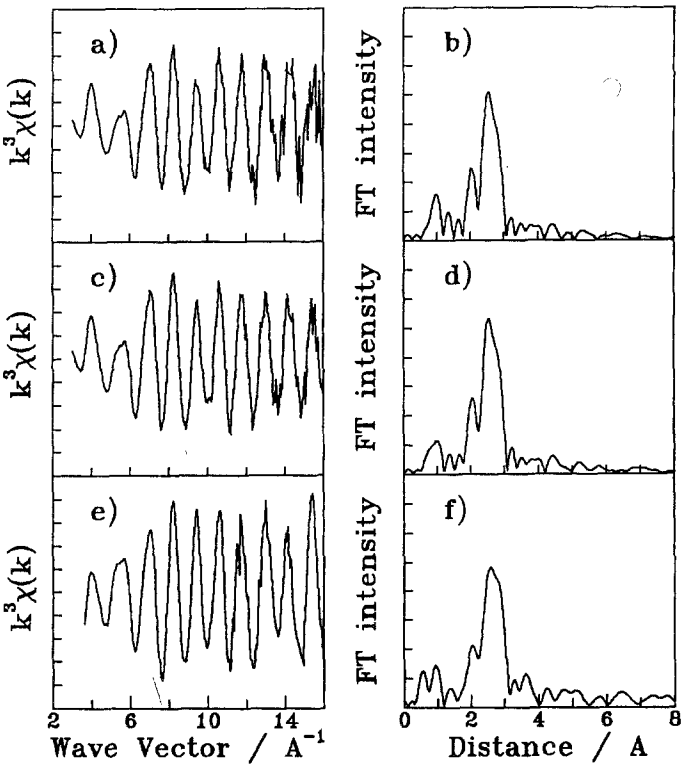

Fig. 1. Normalized Pt L_{III}-edge EXAFS data, $k^3\chi(k)$ vs. k at 300 K and the corresponding Fourier transforms; (a, b) 2.0 wt% Pt/NaY, (c, d) 5.0 wt% Pt/NaY and (e, f) 10.0 wt% Pt/NaY.

Table 1
Structural parameters estimated from Pt L_{III} EXAFS and the Xe/Pt ratio obtained from xenon adsorption on Pt/NaY

Sample	R[a] (nm)	N[b]	Xe/Pt[c]
2.0 wt% Pt/NaY	0.275	5.0 ± 1.2	0.069
5.0 wt% Pt/NaY	0.275	5.9 ± 1.1	0.069
10.0 wt% Pt/NaY	0.276	5.1 ± 1.0	0.066
2 + 8 wt% Pt/NaY[d]	0.276	4.4 ± 1.4	0.073
2.0 wt% Pt/NaY[e]	0.277	11.3 ± 1.1	–

[a] Pt–Pt distance, with ±0.001.
[b] Pt–Pt coordination number, with fitting error bar.
[c] The difference between xenon adsorption isotherms with and without chemisorbed hydrogen, extrapolating from the high-pressure region above 10 kPa to zero pressure.
[d] Prepared by loading 8.0 wt% Pt onto 2.0 wt% Pt/NaY.
[e] Pt network sample reduced at 673 K without the activation.

with a narrow range of 4.9±1.3, which indicates that the average cluster size is independent of the Pt content, within the precision limit for the EXAFS analysis. The error bar is a 95% confidence limit which was obtained statistically for the four small-cluster samples listed in table 1 and two other samples prepared similarly. We have also taken transmission electron micrographs for the Pt/NaY samples, but they have provided no further information than the presence of ~ 1 nm Pt clusters.

Recently, we have proposed a method using xenon adsorption which provides very precise information on the average cluster size for group VIII metals located in supercages of faujasite-type zeolite [8–11]. Fig. 2 shows xenon adsorption isotherms obtained for the application of the xenon adsorption method to 10.0 wt% Pt/NaY for example. The open circle in fig. 2 represents xenon adsorption on the freshly prepared sample without chemisorbed hydrogen at 296 K. The closed circle has been obtained after the sample was equilibrated with 1 atm H_2 for 30 min and subsequently evacuated at 296 K. The difference between xenon adsorption isotherms with and without chemisorbed hydrogen is due to the amount of xenon adsorbed on the clean Pt surface with a heat of adsorption of, e.g., $\Delta H_{ads} \approx 45$ kJ mol^{-1}, while the nearly linear adsorption isotherm obtained after hydrogen chemisorption is due to xenon adsorption on the zeolite support with only $\Delta H_{ads} \approx 23$ kJ mol^{-1}, because the chemisorption of hydrogen hinders the relatively strong adsorption of xenon on the Pt surface. Ryoo et al. measured the heat of adsorption at 296 K by using the Clapeyron equation,

$$-\frac{\Delta H_{ads}}{R} = \left[\frac{\partial \ln P}{\partial(1/T)}\right]_{N_s},$$

where N_s is the total amount of adsorbed xenon measured from the xenon adsorption isotherm at 293, 296, and 299 K [8]. The xenon adsorption on Pt is so strong

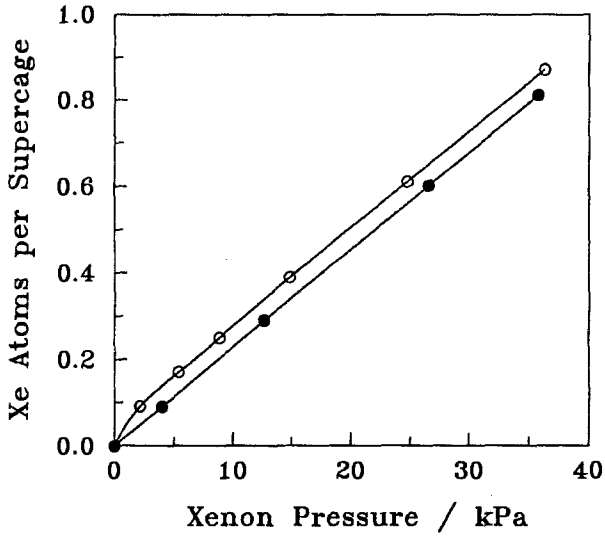

Fig. 2. Xenon adsorption isotherms of 10.0 wt% Pt/NaY sample: (○) fresh; (●) after hydrogen chemisorption, at 296 K.

that the adsorption becomes saturated. The amount of xenon adsorption for saturation has been obtained by extrapolating the difference between the two xenon adsorption isotherms with and without chemisorbed hydrogen, from the pressure range above 10 kPa to zero pressure. Oxygen can be substituted for hydrogen to block the xenon adsorption on Pt cluster. The result is summarized in table 1 in terms of the Xe/Pt ratio.

If the amount of xenon adsorption for saturation on the Pt surface can be assumed to be proportional to the total surface area of Pt exposed to xenon, the adsorbed xenon quantity per metal atom will decrease with increase of the cluster size. Such difference in the xenon adsorption quantity for saturation on metal samples was indeed measured in previous studies on Pd cluster encaged in supercage [9], Pd cluster agglomerated through adjacent supercages [9], and Ru clusters consisting of different numbers of Ru atoms [8,10], which seemed to range from 20 to 50 depending on the Ru content and the reduction temperature. However, the xenon quantity for Pt/NaY remains unchanged within 0.069 ± 0.004 Xe/Pt even when the Pt content has been increased five times from 2.0 to 10.0 wt%, as listed in table 1. Thus, our result from xenon adsorption measurements confirms the conclusion from EXAFS that the average Pt cluster size is almost independent of the Pt content for 2–10 wt% Pt/NaY samples. Here, we may assume that the xenon adsorption quantity for saturation on Pt surface corresponds to a maximum number of xenon atoms that can be in direct contact with the Pt cluster. Then, with use of space-filling chemical models for Pt, Xe and NaY supercage, it is possible to show that a cluster consisting of 50–60 Pt atoms fills the supercage, and the Pt clus-

ter can adsorb up to four xenon atoms on the surface exposed through four apertures of the supercage. In this case, the ratio between the numbers of the adsorbed xenon and Pt atoms becomes to agree with our experimental value, 0.069 ± 0.004 Xe/Pt. The xenon adsorption model used for determination of the number of metal atoms per cluster is described as a function of Xe/metal in our recent publications [8–10].

We have also increased the Pt content of sample by repeating the Pt loading procedure (i.e., ion exchange of $Pt(NH_3)_4^{2+}$, activation, and reduction) on a Pt/NaY sample which was exposed to air after loading Pt cluster by the same procedure. Recent studies using ^{129}Xe NMR and EXAFS for PtCu and PtAg bimetallic clusters supported on NaY zeolite indicated that the Cu and Ag atoms were added (or adsorbed) onto Pt cluster in supercage [11,12]. However, there seems to be no significant interaction between the Pt cluster which was prepared by the first loading treatment and the Pt atoms which were reduced during the second loading, as the Xe/Pt ratio was not considerably decreased by repeating the Pt loading, e.g., by the addition of 8.0 wt% Pt onto 2.0 wt% Pt/NaY. The Pt–Pt coordination number from EXAFS was also unchanged in this case, as summarized in table 1. It seems that a small Pt cluster consisting of 50–60 Pt atoms is obtained either by a single loading or by repeating the loading twice, under our experimental condition. This result is difficult to explain unless the cluster size is distributed over an extremely narrow range. The result from Pt/NaY is in sharp contrast with our earlier report on Ru/NaY which showed wide variation of the xenon per metal ratio, e.g. 0.20–0.08 Xe/Ru among samples with different Ru wt% and those heated at different temperatures [8,10]. There seems to exist significant interaction between Pt and the supercage wall, which can stabilize the cluster size that just fits for a supercage.

There is a remarkable consistency among the Pt–Pt coordination numbers which are obtained from our standard EXAFS analysis for 2–10 wt% Pt/NaY prepared by ion exchange of $Pt(NH_3)_4^{2+}$, calcination, and reduction. However, it is noteworthy that the result is substantially different from 50–60 Pt atoms per cluster which has been estimated from xenon adsorption measurements, as the Pt–Pt coordination number, 4.9 ± 1.3, is compatible with a cluster consisting of only 6–18 Pt atoms packed in face centered cubic structure with a nearly spherical geometry. The difference between EXAFS and xenon adsorption data agrees remarkably with a very recent result obtained by Clausen et al. [13] with use of the molecular dynamic simulation that the standard curve-fitting method seriously underestimates the coordination number for small Cu clusters, mainly due to anharmonic atomic motion in the small particle. Thus, our result from Pt/NaY provides experimental data related to the critical question as to the accuracy of the EXAFS method for the estimation of very small metal cluster sizes.

Nanosize Pt Networks. It is well known in the preparation of Pt/NaY that the Pt atoms form large agglomerates mostly at the external surface of the zeolite crystal if the ion exchanged $Pt(NH_3)_4^{2+}$ is directly reduced with H_2 at high temperature without activation in O_2 [3]. There is a recent report [14] on the formation of large

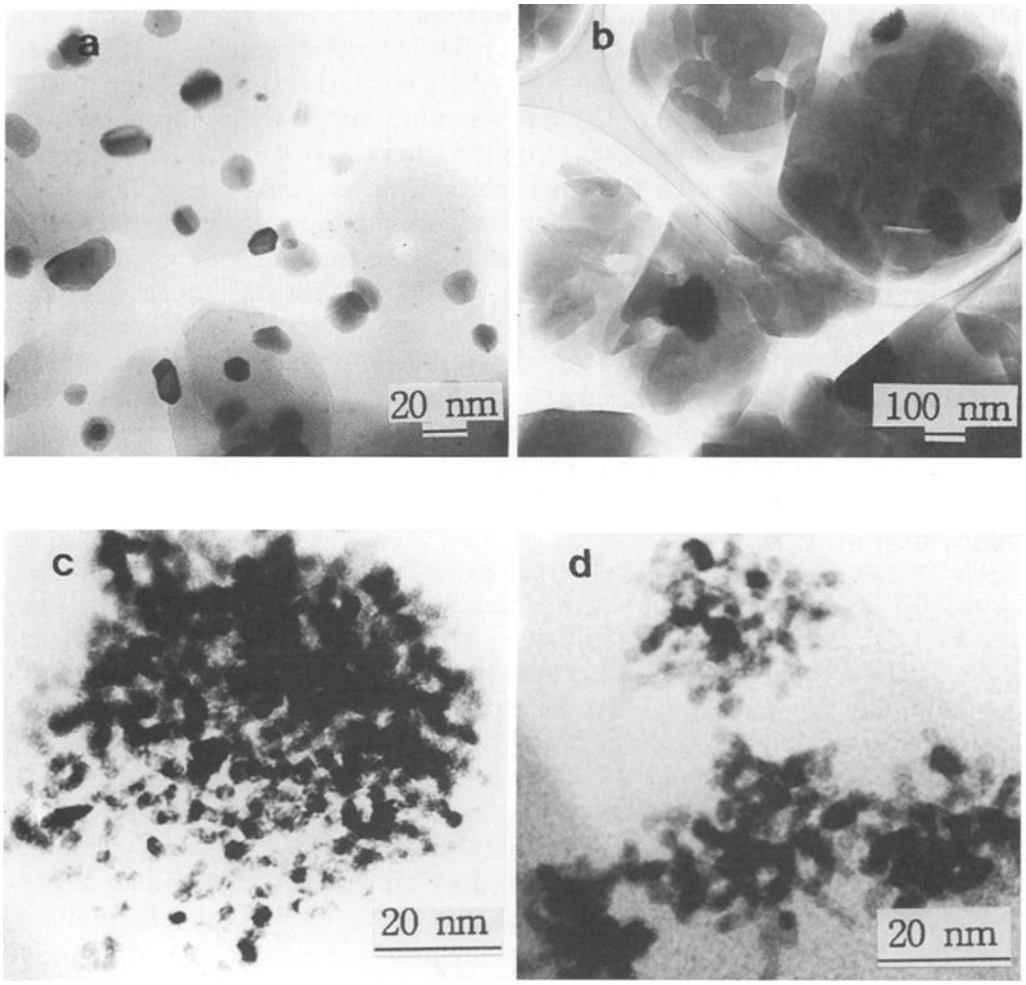

Fig. 3. Transmission electron micrographs for 2.0 wt% Pt/NaY samples taken through the zeolite crystallites. (a) Pt particles of about 30 nm size are located on the external surface of zeolite crystal if the sample is prepared with rapid increase of the reduction temperature from RT to 673 K over 2 h. (b) Pt agglomerates are located inside of the zeolite crystal, near to the external surface, if the sample is prepared with slow increase of the reduction temperature from RT to 673 K over 20 h. (c) Magnification of a large Pt agglomerate in (b). (d) Magnification of a few small Pt agglomerates showing more detailed morphology of the Pt network structure than in (c). Overall thickness of the Pt structure appears to differ in (c) and (d) due to the different sizes.

agglomerates in the vicinity of the external surface, within the zeolite crystal. Our result in fig. 3 agrees with the formation of Pt agglomerates on the external surface if the reduction temperature is increased rapidly, e.g., from RT to 673 K over 2 h [3]. If the reduction temperature is raised very slowly, e.g., over 20 h, the Pt clustering seems to form a network within the zeolite crystal as shown in figs. 3b, 3c and 3d which is similar to the one reported in ref. [14]. The Pt network appears to build

an interesting structure in which quantum-sized wire about 3 nm in diameter is interconnected in a three-dimensional way. The overall dimension of the Pt network ranges from as small as 10 nm to very often larger than 100 nm. In many zeolite crystals, only a single large network structure can be found throughout the entire crystal. In this case, the Pt clustering must have started at a single nucleation site within the zeolite crystal or at the external surface, progressing until all Pt atoms in the zeolite crystal have been agglomerated together. It is also interesting that the Pt network in the micrograph is very often located just underneath an edge or corner of the zeolite crystal. Probably, the Pt network starts formation at a nucleation site on the external surface, growing into the crystal. The formation of such Pt network seems to require a very slow quasi-static process, which fails under rapid increase of the reduction temperature. The growth of the Pt network within the zeolite crystal, rather than the formation of large Pt particles on the external surface, indicates that the Pt network is stabilized by the interaction with the internal surface of zeolite. That is, Pt and NaY zeolite seem to have significant metal–support interaction.

The transmission electron micrographs in fig. 3 show that the shape of the zeolite crystal has not been changed by the formation of Pt network within the crystal. The Pt–Pt coordination number estimated from EXAFS will be useful to distinguish if the Pt network of about 3 nm thick has been formed with or without breaking the zeolite framework between the supercages containing Pt atoms. If the Pt agglomerate is formed through adjacent supercages with no framework damage, the Pt–Pt coordination number will not be considerably greater than that of a small Pt cluster filling supercage, because only a few Pt atoms will contact through the supercage aperture. However, such was not the result as the coordination number listed in table 1 is about 11. The zeolite framework between adjacent supercages should be broken to accommodate for such Pt network, although the shape of zeolite crystal has been maintained.

Acknowledgement

RR acknowledges support from the Korea Science and Engineering Foundation. The EXAFS experiment was supported by Photon Laboratory (Proposal No. 89-147) and Pohang Accelerator Laboratory.

References

[1] P.A. Jacobs, in: *Metal Microstructures in Zeolites*, Vol. 12, eds. P.A. Jacobs, N.I. Jaeger, P. Jiru and G. Schulz-Ekloff (Elsevier, Amsterdam, 1982) p. 71.
[2] R.A. Dalla-Betta and M. Boudart, in: *Proc. 5th Int. Congr. on Catalysis*, Vol. 2, ed. J. Hightower (North-Holland, Amsterdam, 1973) p. 1329.
[3] P. Gallezot, Catal. Rev.-Sci. Eng. 20 (1979) 121.
[4] M. Boudart, M.G. Samant and R. Ryoo, Ultramicroscopy 20 (1986) 125.

[5] B.F. Chmelka, R. Ryoo, S.B. Liu, L.-C. de Menorval, C.J. Radke, E.E. Petersen and A. Pines, J. Am. Chem. Soc. 110 (1988) 4465.
[6] B.F. Chmelka, L.-C. de Menorval, R. Csencsits, R. Ryoo, S.B. Liu, C.J. Radke, E.E. Petersen and A. Pines, in: *Structure and Reactivity of Surfaces*, Vol. 48, eds. C. Morterra, A. Zecchina and G. Costa (Elsevier, Amsterdam, 1989) p. 269.
[7] J.-G. Kim, PhD Dissertation, KAIST, Korea (1992).
[8] R. Ryoo, S.J. Cho, C. Pak, J.-G. Kim, S.-K. Ihm and J.Y. Lee, J. Am. Chem. Soc. 114 (1992) 76.
[9] J.-G. Kim, S.-K. Ihm, J.Y. Lee and R. Ryoo, J. Phys. Chem. 95 (1991) 8546.
[10] S.J. Cho, S.M. Jung, Y.G. Shul and R. Ryoo, J. Phys. Chem. 96 (1992) 9922.
[11] D.H. Ahn, J.S. Lee, M. Nomura, W.M.H. Sachtler, G. Moretti, S.I. Woo and R. Ryoo, J. Catal. 133 (1992) 191.
[12] R. Ryoo, C. Pak and S.J. Cho, *Proc. 7th Int. Conf. on XAFS*, Kobe, August 1992, Japan. J. Appl. Phys., in press.
[13] B.S. Clausen, J. Gråbæk, H. Topsøe, L.B. Hansen, P. Stoltze and J.K. Nørskov, *Proc. 7th Int. Conf. on XAFS*, Kobe, August 1992, Japan. J. Appl. Phys., in press.
[14] P. Gallezot, A. Giroir-Fendler and D. Richard, Catal. Lett. 5 (1990) 169.